2-Amino-*N*-pyrimidin-4-ylacetamides as A_{2A} Receptor Antagonists: 2. Reduction of hERG Activity, Observed Species Selectivity, and Structure−Activity Relationships

Deborah H. Slee,*[,‡] Manisha Moorjani,[‡] Xiaohu Zhang,[‡] Emily Lin,[‡] Marion C. Lanier,[‡] Yongsheng Chen,[‡] Jaimie K. Rueter,[‡] Sandra M. Lechner,[⊥] Stacy Markison,[⊥] Siobhan Malany,[#] Tanya Joswig,[⊥] Mark Santos,[#] Raymond S. Gross,[†] John P. Williams,[‡] Julio C. Castro-Palomino,[||] María I. Crespo,[||] Maria Prat,[||] Silvia Gual,[||] José-Luis Díaz,[||] Kayvon Jalali,[§] Yang Sai,[§] Zhiyang Zuo,[§] Chun Yang,[§] Jenny Wen,[§] Zhihong O'Brien,[§] Robert Petroski,[⊥] and John Saunders[‡]

Departments of Medicinal Chemistry, Pharmacology and Lead Discovery, Neuroscience, Chemical Development, and Preclinical Development, Neurocrine Biosciences, 12790 El Camino Real, San Diego, California 92130, and Almirall Research Center, Almirall, Ctra. Laureà Miró, 408-410, E-08980 St. Feliu de Llobregat, Barcelona, Spain

Received September 20, 2007

Previously we have described a series of novel A_{2A} receptor antagonists with excellent water solubility. As described in the accompanying paper, the antagonists were first optimized to remove an unsubstituted furyl moiety, with the aim of avoiding the potential metabolic liabilities that can arise from the presence of an unsubstituted furan. This effort identified a series of potent and selective methylfuryl derivatives. Herein, we describe the further optimization of this series to increase potency, maintain selectivity for the human A_{2A} vs the human A_1 receptor, and minimize activity against the hERG channel. In addition, the observed structure−activity relationships against both the human and the rat A_{2A} receptor are reported.

Introduction

Parkinson's disease (PD) is a debilitating disorder for which there have been few novel treatments developed in recent years. To date, the market is dominated by treatments that enhance dopaminergic activity either via administration of dopamine agonists or by dopamine replacement therapy with levodopa (L-dopa). These treatments are not without side effects, which include nausea, vomiting, dry mouth, confusion, hallucinations, and somnolence (including sleep attacks). Furthermore, as the disease progresses, the efficacy of these drugs can diminish and the development of motor fluctuations and peak dose dyskinesias are common.[1]

A_{2A} receptor antagonists offer a new approach to the treatment of PD that might avoid some of these side effects. Clinical trials evaluating the motor effects observed in PD patients exhibiting motor fluctuations and peak dose dyskinesias have validated the use of A_{2A} antagonists as an adjunct therapy to neurotransmitter replacement in this patient population.[2] There is also the potential for A_{2A} receptor antagonists to be effective on movement dysfunction in early stage patients, either alone or with reduced doses of dopamine agonists and/or L-dopa.[3] In addition, the A_{2A} receptor has been shown to play a role in mediation of arousal and A_{2A} antagonists may be able to counter the somnolent effect of these dopaminergic therapies.[4] Perhaps most importantly, there is a growing body of preclinical evidence that A_{2A} receptor antagonists demonstrate neuroprotective properties that may offer protection against the development of dyskinesias and may ultimately result in a slowing of the progression of the disease.[5]

In the accompanying paper we described the SAR that led to the identification of compound **1**. Further profiling of this lead identified compound **1** as a weak inhibitor of the hERG channel as measured by electrophysiology. In addition, we found that this series of A_{2A} receptor antagonists exhibited distinct differences in potency between the human and rat adenosine A_{2A} receptors, which helped to explain the limited efficacy observed in the rodent. The existence of different structure–activity relationships (SARs) for the human and rat A_{2A} receptors is rarely discussed in the literature. In this case we believe that the reduced activity against the rat receptor inhibited our ability to demonstrate efficacy at reasonable doses for many analogues in this series. Herein, we describe the lead optimization of this series and the SAR against both the human and rat A_{2A} receptors.

Chemistry

In the accompanying paper[6] the synthesis and characterization of compound **1**, which is derived from the key intermediate **2**, was described. A number of analogues of compound **1** were synthesized according to the procedures outlined in Schemes 1 and 2.

Three main approaches were used to synthesize the desired analogues as follows. The synthesis of compound **4** was achieved through attaching the side chain via acylation of intermediate **2**, with the acyl chloride generated from treatment of 4-carboxymethylpiperidine-1-carboxylic acid *tert*-butyl ester with oxalyl chloride to give intermediate **3**. Intermediate **3** was then deprotected with TFA followed by reductive amination to install a methyl group to give compound **4**. Analogues **1** and **6–18** were derived from key intermediate **5**. Key intermediate **5** was synthesized via treatment of compound **2** with chloroacetyl chloride. Intermediate **5** was then treated with the desired amine to displace the chlorine to give the final products **1** and **6–18**. Alternatively, intermediate **5** could be treated with the appropriate Boc-protected amine to give intermediates **19a−e**. In a manner similar to the synthesis of compound **4** from intermediate **3**, intermediates **19a−e** were then deprotected via

* To whom correspondence should be addressed. Phone: 858-617-7849. Fax: 858-617-7619. E-mail: dslee@neurocrine.com.

‡ Department of Medicinal Chemistry, Neurocrine Biosciences.

⊥ Department of Neuroscience, Neurocrine Biosciences.

Department of Pharmacology and Lead Discovery, Neurocrine Biosciences.

† Department of Chemical Development, Neurocrine Biosciences.

|| Almirall Research Center.

§ Department of Preclinical Development, Neurocrine Biosciences.

10.1021/jm701187w CCC: $40.75
Published on Web 02/29/2008

Scheme 1[a]

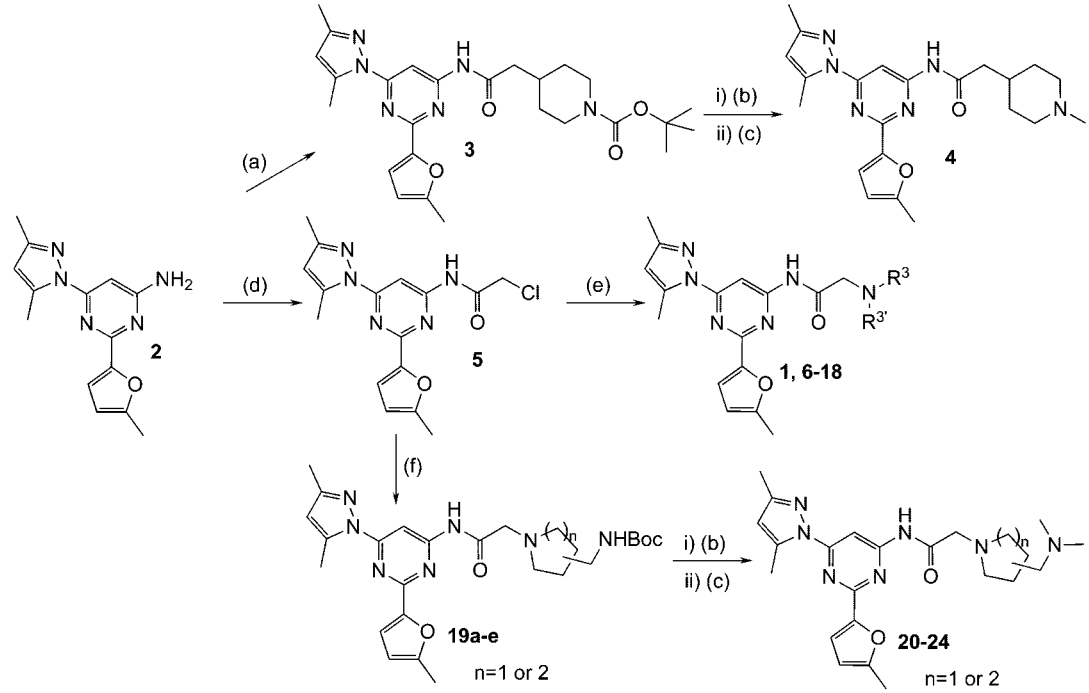

[a] Reagents and conditions: (a) 1-Boc-piperidine-4-ylacetic acid, oxalyl chloride, catalyst DMF, THF, evaporate, then DCM, pyridine, room temp, 4 h, 98%; (b) TFA, DCM, room temp, 1 h; (c) BH_3·pyridine, HCOH, catalyst acetic acid, ethanol, 18 h, 22–79%; (d) chloroacetyl chloride, pyridine, DCM, room temp, 2 h, 100%; (e) amine, DCM, DIPEA, room temp, 6−12 h, 17–92%; (f) Boc-protected diamine, DMF, TBAI, 70–90%.

Scheme 2[a]

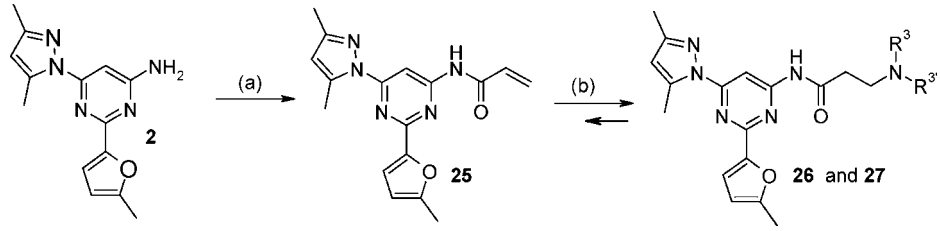

[a] (a) Acryloyl chloride, pyridine, DCM, room temp, 6–12 h, 80%; (b) primary or secondary amine, DMF, room temp, 18 h, 75–78%.

treatment with TFA, followed by reductive amination to give the methylated analogues **20–24** (Table 1).

Homologated analogues **26** and **27** were synthesized by reaction of intermediate **2** with acryloyl chloride to give intermediate **25**, followed by Michael addition with the appropriate amine.

Results and Discussion

Compound **1** is a potent human A_{2A} (hA_{2A}) receptor antagonist (K_i = 12 nM). When profiled in secondary assays, compound **1** did not show any inhibition of the major CYP enzymes (CYP2D6 or 3A4) but was found to have activity against the hERG (human ether-a-go-go related gene) channel (IC_{50} = 950 nM, hERG patch-clamp). In addition, the activity against the rat A_{2A} (rA_{2A}) receptor was found to be on the order of 10-fold less than for the human A_{2A} receptor. Because a rat efficacy model was used to evaluate compounds, it was necessary to track the activity of analogues against both human and rat A_{2A} receptors.

The available SAR around the R^3 side chain (Figure 1) led us to believe that the basic amine containing side chain was responsible for the hERG activity. This SAR had not been fully explored, and optimization of this side chain was undertaken with the aim of increasing selectivity for A_{2A} vs the hERG channel. Various techniques for reducing hERG activity were explored, including changing the distance between the amino moieties, changing the shape of the side chain and distance between the amine and the pyrimidine moiety, and varying the pK_a of the amine moieties.[7] The SAR around the amino containing side chains (R^3, Figure 1) for this series is summarized in Table 1. It was found that extending the methyl on the piperazine of lead compound **1** to ethyl to give compound **6** maintained potency and significantly enhanced selectivity for hA_{2A} vs human A_1 (hA_1) to 171-fold. Enlarging the ring from a piperazine to a homopiperazine as in analogue **7** again maintained potency (hA_{2A} K_i = 10 nM) and enhanced selectivity against hA_1 to 210-fold but also increased hERG activity (IC_{50} = 285 nM). Further exploration by varying the relative positions, spacing, and shape of the amino side chain gave interesting results. Significant enhancement of potency was observed when the distance between the two nitrogen atoms was increased, as exemplified by compound **21** (hA_{2A} K_i = 1.5 nM). Interestingly, this increase in potency was stereospecific, with the *S*-isomer **21** being more potent but less selective (hA_{2A} K_i = 1.5 nM, hA_1/hA_{2A} 47-fold) than the *R*-isomer **20** (hA_{2A} K_i = 10 nM, hA_1/hA_{2A} 89-fold). It was possible to remove the chirality to give compound **22** and maintain potency and improve selectivity (hA_{2A} K_i = 2.9 nM, hA_1/hA_{2A} 131-fold). When compound **22**

Table 1[d]

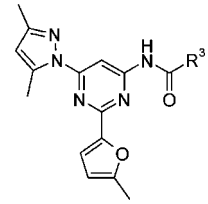

		K_i (nM) ± SEM				hERG
Compound	R^3	hA_{2A}[a]	hA_1[b]	hA_1/hA_{2A}	rA_{2A}[c]	IC_{50} (nM)
1	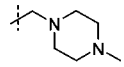	12 ± 2	850 ± 230	71	131.3 ± 0.3	950
6	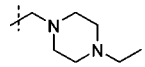	11 ± 1	1880 ± 130	171	270 ± 170	ND
7	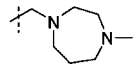	10 ± 4	2100 ± 700	210	46.7 ± 0.2	285
20	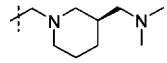	10 ± 1	890 ± 53	89	87 ± 1	ND
21	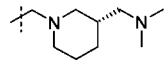	1.5 ± 0.1	71 ± 9	47	14 ± 1	ND
22	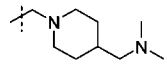	2.9 ± 0.3	380 ± 16	131	25 ± 2	1670
8	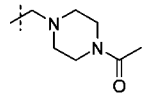	3.6 ± 0.1	540 ± 40	150	170 ± 10	ND
9	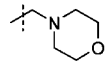	5.7 ± 0.2	500 ± 40	88	430 ± 50	ND
10	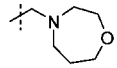	6 ± 2	630 ± 80	105	230 ± 90	ND
11	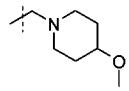	15 ± 2	1210 ± 80	81	1600 ± 170	ND
4	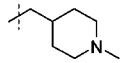	5.4 ± 0.4	1020 ± 50	189	103 ± 6	4170
12		8.6 ± 0.3	347 ± 1	40	ND	ND
13	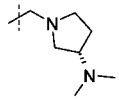	3.7 ± 0.6	940 ± 66	254	160 ± 40	600
14	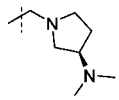	4.0 ± 0.2	262 ± 3	66	ND	ND
15	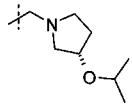	86 ± 3	2300 ± 100	27	ND	ND

Table 1. Continued

		K_i (nM) ± SEM				hERG
Compound	R^3	hA_{2A}[a]	hA_1[b]	hA_1/hA_{2A}	rA_{2A}[c]	IC_{50} (nM)
16	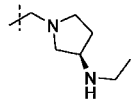	3.8 ± 0.5	270 ± 30	71	ND	ND
17	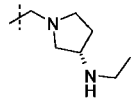	2.5 ± 0.3	370 ± 20	148	37 ± 7	420
18	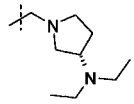	4.4 ± 0.4	2600 ± 300	591	155 ± 9	ND
23	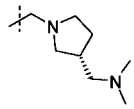	11 ± 5	550 ± 250	50	34 ± 4	1860
24	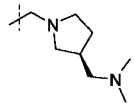	2.1 ± 0.1	220 ± 10	105	27.8 ± 0.2	1010
26		2.1 ± 0.2	210 ± 10	100	43 ± 2	650
27	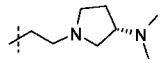	2.4 ± 0.1	630 ± 80	263	41 ± 3	2280

[a] Displacement of specific [^{3}H]-ZM 241385 binding at human A_{2A} receptors expressed in HEK293 cells. [b] Displacement of specific [^{3}H]-DPCPX binding at human A_1 receptors expressed in HEK293 cells. [c] Displacement of specific [^{3}H]-ZM 241385 binding at rat A_{2A} receptors expressed in CHO cells. [d] Data are expressed as mean values of at least two runs ± SEM. ND: not determined.

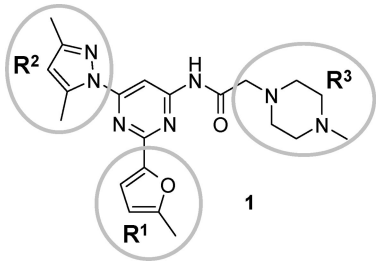

Figure 1

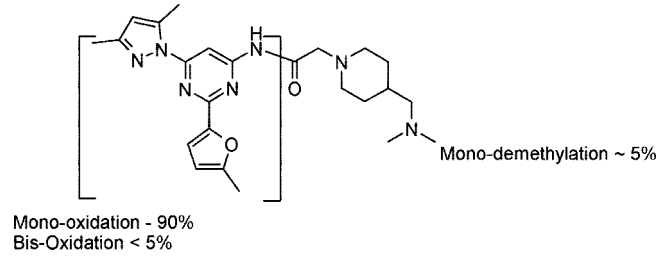

Figure 2. Metabolites of compound **22**, after incubation with human liver microsomes (tentative assignment of peaks observed by LCMS). When incubated with human liver microsomes plus GSH (10 mM), no detectable amount of GSH adducts were observed.

was profiled in the hERG assay, the IC_{50} was found to be 1670 nM, a potency similar to that of the lead compound **1**, but the selectivity for the hA_{2A} receptor over the hERG channel was improved from 79-fold to 576-fold because of the increased potency of compound **22** against the A_{2A} receptor. In vitro metabolite identification via LCMS after incubation of **22** in human liver microsomes (HLM) showed that the major metabolite was mono-oxidation somewhere on the aromatic system (Figure 2), possibly on one of the methyl groups. As expected, no downstream metabolites resulting from metabolism of the furyl moiety were observed, indicating that the methyl group had blocked the metabolism observed previously when the furan was unsubstituted.[6] In addition, no glutathione (GSH) adducts were observed when the compound was incubated with HLM in the presence of GSH, further supporting the absence of electrophilic reactive metabolites.

The basicity of the more basic nitrogen (distal to the pyrimidine moiety) in the side chain of compound **1** could be attenuated without a dramatic effect on binding, as illustrated by the amide analogue **8**. This distal amine could also be replaced by oxygen as in the morpholine analogue **9** and the homomorpholine compound **10**. From cassette PK studies in rodent, however, the brain levels were poor for these analogues, indicating a reduced capacity to cross the blood−brain barrier. Moving the oxygen out of the ring as in the methoxypiperidine analogue **11** resulted in a loss in potency against the human A_{2A} receptor and a dramatic loss in potency against the rat A_{2A} receptor. A series of pyrrolidine analogues were also synthesized, and it was found that the *S*-dimethylaminopyrrolidine analogue **13** was potent and selective, as were a number of aminopyrrolidine analogues as exemplified by compounds **13**–**18**. Unfortunately, for the pyrrolidine analogues tested, the potency at the hERG channel increased to less than 1 μM, as illustrated by compounds **13** and **17**. Increasing the distance between the two nitrogen atoms in the pyrrolidine series, as in

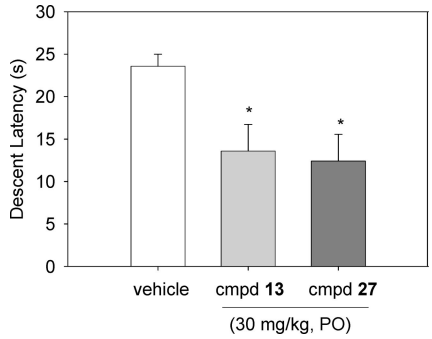

Figure 3. Effect of compounds **13** and **27** (2 h after dose) on mean descent latency (± standard error) in seconds on haloperidol-induced catalepsy in the bar test. The vehicle bar represents the mean and standard error from both experiments combined: (∗) vehicle versus treated rats, $p < 0.05$.

Table 2[a]

compd	$K_i \pm$ SEM (nM) hA_{2A}[b]	$K_i \pm$ SEM (nM) rA_{2A}[c]	exposure[d] in rat brain (ng/g)
13	3.7 ± 0.6	160 ± 40	1900
27	2.4 ± 0.1	41 ± 3	250

[a] Data are expressed as mean values of at least two runs ± SEM. [b] Displacement of specific [^{3}H]-ZM 241385 binding at human A_{2A} receptors expressed in HEK293 cells. [c] Displacement of specific [^{3}H]-ZM 241385 binding at rat A_{2A} receptors expressed in CHO cells. [d] At 2 h after dosing with a 30 mg/kg oral (po) dose.

compounds **23** and **24**, reduced hERG activity while maintaining the desired potency and selectivity for the hA_{2A} receptor.

Further exploration of the piperazine series to investigate the importance of the piperazine nitrogen atom of compound **1** nearest the pyrimidine found that replacement with a carbon to give the carbon-linked methylpiperidine analogue **4** gave a potent and selective molecule, which implies that the distal amine is most important for potency and selectivity. Interestingly the hERG activity for this compound was also attenuated to 4170 nM. In addition, as typically seen for this series, compound **4** was on the order of 20-fold less active at the rat than the human A_{2A} receptor.

A limited set of compounds were made where the linker between the acyl and amino moieties was extended. Initially these compounds looked very promising and two of the most potent and selective analogue compounds **26** and **27** are shown at the bottom of Table 1. These compounds were stable enough for in vitro and in vivo evaluation but showed signs of chemical instability on storage, arising from a retro-Michael reaction that gives the corresponding acrylate precursor (see Scheme 2). Because of this instability, this subseries was not pursued further.

In general, compounds in this series did not exhibit robust efficacy in rodent at doses of less than 30 mg/kg. It is believed that this is largely explained by a lack in potency at the rat A_{2A} receptor. However, in some cases it was possible to demonstrate efficacy at doses of 30 mg/kg. Two such examples are compounds **13** (hA_{2A} $K_i = 3.7$ nM) and **27** (hA_{2A} $K_i = 2.4$ nM), which were evaluated in the haloperidol-induced catalepsy (HIC) assay[8] and demonstrated significant efficacy at 30 mg/kg po 2 h after dosing, as shown in Figure 3. These compounds were 20 to 40-fold less active against the rat receptor (compound **13**, rA_{2A} $K_i = 160$ nM and compound **27**, rA_{2A} $K_i = 41$ nM, Table 2), which in combination with exposure in the brain helped to explain that relatively high doses were required to show efficacy for these compounds.

Conclusion

We have developed a series of potent and selective adenosine A_{2A} receptor antagonists that incorporate amine containing side chains that confer good selectivity and potency in addition to instilling good physical properties for drug development. The presence of these amines, however, made the series active against the hERG channel. SAR studies around the amine containing side chain identified compounds with potent A_{2A} receptor activity and reduced activity against the hERG channel. Removal of one of the amine moieties to give compound **4** maintained potency and selectivity for the adenosine A_{2A} receptor, and the activity against hERG was reduced to 4170 nM (now 772-fold selective for the hA_{2A} receptor vs the hERG channel). In vitro metabolism studies on a representative compound (**22**) indicated that there were no reactive metabolites formed from the methylfuran. Demonstration of efficacy in the rodent was confounded by lack of potency against the rat receptor. It was possible to demonstrate in vivo efficacy for some members of this series in a rat model of haloperidol induced catalepsy, at relatively high doses of 30 mg/kg. This indication of efficacy increases confidence that these compounds should be efficacious in higher species where the potency is significantly higher.

Experimental Section

Reagents, starting materials, and solvents were purchased from commercial suppliers and used as received. Concentration refers to evaporation under vacuum using a Büchi rotatory evaporator. Reaction products were purified, when necessary, by flash chromatography on silica gel (40–63 μm) with the solvent system indicated. Spectroscopic data were recorded on a Varian Mercury 300 MHz spectrometer, Bruker DPX-250 spectrometer, or Bruker Avance 500 MHz spectrometer. The elemental analysis was done by Robertson Microlit Laboratory, Madison, NJ. Melting points were recorded on a Büchi 535 apparatus. HPLC−MS method 1 was as follows: platform, Agilent 1100 series equipped with an autosampler, a UV detector (220 and 254 nm), a MS detector (APCI); HPLC column, YMC ODS AQ, S-5, 5 μm, 2.0 mm × 50 mm cartridge; HPLC gradient, 1.0 mL/min from 10% acetonitrile in water to 90% acetonitrile in water in 2.5 min, maintaining 90% for 1 min. Both acetonitrile and water have 0.025% TFA. Analytical HPLC−MS method 2 was as follows: platform, Agilent 1100 series equipped with an autosampler, a UV detector (220 and 254 nm), a MS detector (APCI); HPLC column, Phenomenex Synergi-Max RP, 2.0 mm × 50 mm column; HPLC gradient, 1.0 mL/min from 5% acetonitrile in water to 95% acetonitrile in water in 13.5 min, maintaining 95% for 2 min. Both acetonitrile and water have 0.025% TFA. Analytical HPLC−MS method 3 was as follows: platform, Agilent 1100 series equipped with an autosampler, a UV detector (220 and 254 nm), a MS detector (APCI), and Berger FCM 1200 CO_2 pump module; HPLC column, pyridine PYR 60A, 6 μm, 4.6 mm × 150 mm column; HPLC gradient, 4.0 mL/min, 120 bar, from 10% methanol in supercritical CO_2 to 60% methanol in supercritical CO_2 in 1.67 min, maintaining 60% for 1 min. Backpressure was regulated at 140 bar. Analytical HPLC−MS method 4 was as follows: platform, Dionex equipped with an autosampler, a UV detector (220 and 254 nm), a MS detector (APCI); HPLC column, Phenomenex C18 4.6 mm × 150 mm; HPLC gradient, 2.5 mL/min from 5% acetonitrile in water to 90% acetonitrile in water in 9.86 min, 12.30 min run. Both acetonitrile and water have 0.04% NH_4OH. Analytical HPLC−MS method 5 was as follows: platform, Agilent 1100 series equipped with an autosampler, a UV detector (220 and 254 nm), a MS detector (APCI); HPLC column, Phenomenex Fusion RP, 2.0 mm × 50 mm column; HPLC gradient, 1.0 mL/min. Solvent C is 6 mM ammonium formate in water, and

solvent D is 25% acetonitrile in methanol. The gradient runs from 5% D (95% C) to 95% D (5% C) in 6.43 min with a 1.02 min hold at 95% D followed by a return and hold at 5% D for 1.52 min. Analytical HPLC−MS method 6 was as follows: Platform, Agilent equipped with an autosampler, a UV detector (220 and 254 nm), a MS detector (APCI); HPLC column, Waters XTerraMS C18, 3.0 mm × 250 mm; HPLC gradient, 1.0 mL/min from 10% acetonitrile in water to 90% acetonitrile in water in 46 min, maintaining 90% for 7.0 min. Both acetonitrile and water have 0.025% TFA. Analytical HPLC−MS method 7 was as follows: platform, Agilent equipped with an autosampler, a UV detector (220 and 254 nm), a MS detector (APCI); HPLC column, Waters XTerraMS C18, 3.0 mm × 250 mm; HPLC gradient, 1.0 mL/min from 10% acetonitrile in water to 90% acetonitrile in water in 46 min, maintaining 90% for 7.0 min. Acetonitrile has 0.1% NH_4OH, and water has 0.05% NH_4OH. Preparative HPLC−MS was as follows: platform, Dionex equipped with a Gilson 215 autosampler/fraction collector, UV detector, and a Dionex MSQ mass detector; HPLC column, Phenomenex Synergy Max-RP, 21.2 mm × 50 mm; HPLC gradient, 35 mL/min, 5% acetonitrile in water to 95% acetonitrile in water in 17.7 min. Both acetonitrile and water have 0.05% TFA.

6-(3,5-Dimethylpyrazol-1-yl)-2-(5-methylfuran-2-yl)pyrimidin-4-ylamine (2). Intermediate **2** was prepared according to the methods described in the accompanying paper.

Synthesis of *N*-[6-(3,5-Dimethylpyrazol-1-yl)-2-(5-methylfuran-2-yl)pyrimidin-4-yl]-2-(1-methylpiperidin-4-yl)acetamide (4). To THF (10 mL) were added 1-Boc-piperidine-4-ylacetic acid (540 mg, 2.2 mmol, 1 equiv), followed by oxalyl chloride (300 mg, 0.24 mmol, 1.1 equiv) and a few drops of DMF. The reaction mixture was stirred under nitrogen at room temperature for 1 h and concentrated under vacuum to dryness. The resulting 4-chlorocarbonylmethylpiperidine-1-carboxylic acid *tert*-butyl ester was dissolved in dichloromethane (10 mL), and intermediate **2** (300 mg, 0.5 equiv) was added, followed by pyridine (150 mg). The mixture was stirred at room temperature for 4 h. The reaction was then quenched by addition of saturated sodium bicarbonate (50 mL), extracted with dichloromethane (2 × 50 mL), the organic layers were combined, dried (Na_2SO_4), concentrated, and purified by silica gel column using 40% ethyl acetate in hexane to give 4-{[6-(3,5-dimethylpyrazol-1-yl)-2-(5-methylfuran-2-yl)pyrimidin-4-ylcarbamoyl]methyl}piperidine-1-carboxylic acid *tert*-butyl ester **3** as clear thick oil (540 mg, 98%). LCMS-1: t_R = 3.28 (90%, crude mixture). MS: *m/z* 495 $[M + H]^+$, expected 495 $[M + H]^+$. Compound **3** was dissolved in dichloromethane (10 mL) followed by addition of TFA (10 mL). The mixture was stirred at room temperature for 1 h, and the solvent was removed by nitrogen flow to give deprotected **3** as a clear oil, which was used without further purification (LCMS-1: t_R = 2.32 (95%, crude). MS: *m/z* 395 $[M + H]^+$). Deprotected **3** was dissolved in EtOH (10 mL), followed by addition of formaldehyde (2 mL, 30% in water), acetic acid (10 drops), and borane−pyridine (0.2 mL). The mixture was stirred at room temperature overnight. The reaction was quenched by addition of 1 M HCl (50 mL) with stirring for 10 min, neutralized by addition of saturated sodium bicarbonate, and extracted with dichloromethane (2 × 25 mL). The organic layers were combined, dried (Na_2SO_4), concentrated, and purified by silica gel column using 5% methanol in dichloromethane. Compound **4** was obtained as a clear oil (350 mg, 79%). ^{1}H NMR (300 MHz, $CDCl_3$): δ 8.49 (s, 1H), 8.03 (s, 1H), 7.16 (d, J = 3, 1H), 6.17 (d, J = 3, 1H), 6.01 (s, 1H), 2.83–2.87 (m, 2H), 2.76 (s, 3H), 2.45 (s, 3H), 2.83–2.87 (m, 2H), 2.31 (d, J = 6, 1H), 2.28 (s, 3H), 2.27 (s, 3H), 1.91–1.95 (m, 2H), 1.77–1.81 (m, 2H), 1.33–1.38 (m, 2H). LCMS-6: t_R = 19.79. LCMS-7: t_R = 32.4. MS: *m/z* 409 $[M + H]^+$, expected 409 $[M + H]^+$. A portion of the product was converted to HCl salt. Anal. ($C_{22}H_{28}N_6O_2 \cdot 2HCl \cdot C_2H_6O$) C, H, N.

General Method for Final Compounds 1 and 6–18. To 5 mL of dichloromethane were added compound **2** (0.3 g 1.3 mmol), chloroacetyl chloride (0.22 g, 0.20 mmol, 1.5 equiv), and pyridine (0.16 g). The reaction mixture was stirred at room temperature for 2 h. The reaction was quenched with saturated sodium bicarbonate (5 mL) and extracted with dichloromethane (3 × 15 mL). The organic layers were combined and dried (Na_2SO_4), then concentrated to give 2-chloro-*N*-[6-(3,5-dimethylpyrazol-1-yl)-2-(5-methylfuran-2-yl)pyrimidin-4-yl]acetamide **5** as a yellow solid (0.4 g, 100% crude yield), which used without purification in the next subsequent reaction. LCMS-1: t_R = 2.82 (96%). MS: *m/z* 346 $[M + H]^+$, expected 346 $[M + H]^+$. To dichloromethane (10 mL) were added intermediate **5** (1.6 g, 5.3 mmol), DIPEA (1.85 mL, 10.6 mmol, 2.0 equiv) and the appropriate amine (2.0 equiv). The reaction mixture was stirred at room temperature overnight. The reaction was quenched water (5 mL) and extracted with dichloromethane (3 × 15 mL). The organic layers were combined and dried (Na_2SO_4), then concentrated. The residue was purified either by column chromatography on silica gel (DCM with methanol gradient from 0 to 5%) to give the free base (or the HCl salt if converted via treatment with HCl in ether) or by HPLC (TFA salt).

***N*-[6-(3,5-Dimethylpyrazol-1-yl)-2-(5-methylfuran-2-yl)pyrimidin-4-yl]-2-(4-methylpiperazin-1-yl)acetamide (1).** Intermediate **5** was reacted with 4-methylpiperazine according to the above general procedure. The product was purified by HPLC to give **1** as a white solid (82%). ^{1}H NMR (free base) (CD_3OD): δ 8.42 (s, 1H), 7.20 (d, J = 3.3, 1H), 6.26 (dd, J = 3.0, 0.9, 1H), 6.13 (bs, 1H), 3.28 (s, 2H), 2.76 (s, 3H), 2.58–2.76 (m, 8H), 2.43 (s, 3H), 2.35 (s, 3H), 2.27 (s, 3H). LCMS-2: t_R = 5.27. LCMS-6: t_R = 19.17. MS: *m/z* 410 $[M + H]^+$, expected 410 $[M + H]^+$.

***N*-[6-(3,5-Dimethylpyrazol-1-yl)-2-(5-methylfuran-2-yl)pyrimidin-4-yl]-2-(4-ethylpiperazin-1-yl)acetamide (6).** Intermediate **5** was reacted with 4-ethylpiperazine according to the above general procedure. The product was purified by HPLC to give **6** as a light-brown oil (70%). LCMS-2: t_R = 5.34. LCMS-4: t_R = 9.73 (98%). MS: *m/z* 424 $[M + H]^+$, expected 424 $[M + H]^+$.

***N*-[6-(3,5-Dimethylpyrazol-1-yl)-2-(5-methylfuran-2-yl)pyrimidin-4-yl]-2-(4-methyl[1,4]diazepan-1-yl)acetamide (7).** Intermediate **5** was reacted with *N*-methylhomopiperazine according to the above general procedure. The product was purified by column on silica gel with DCM/methanol, 90/10, to give **7** as a white solid when converted to the HCl salt (45%). LCMS-2: t_R = 4.96. LCMS-5: t_R = 5.70. MS: *m/z* 424 $[M + H]^+$, expected 424 $[M + H]^+$.

2-(4-Acetylpiperazin-1-yl)-*N*-[6-(3,5-dimethylpyrazol-1-yl)-2-(5-methylfuran-2-yl)pyrimidin-4-yl]acetamide (8). Intermediate **5** was reacted with 4-acetylpiperazine according to the above general procedure. The product was purified by HPLC to give **8** as a light-brown oil (70%). LCMS-2: t_R = 5.17. LCMS-5: t_R = 5.86. MS: *m/z* 438 $[M + H]^+$, expected 438 $[M + H]^+$.

***N*-[6-(3,5-Dimethylpyrazol-1-yl)-2-(5-methylfuran-2-yl)pyrimidin-4-yl]-2-morpholin-4-ylacetamide (9).** Intermediate **5** was reacted with 4-acetylpiperazine according to the above general procedure. The product was purified by HPLC to give **9** as the TFA salt (light-brown oil, 85%). ^{1}H NMR (300 MHz, DMSO-d_6): δ 8.33 (bs, 1H), 7.24 (d, J = 3.3, 1H), 6.38 (dd, J = 0.9, 3.3, 1H), 6.24 (s, 1H), 4.3 (brm, 2H), 3.87 (brm, 4H), 2.74 (s, 3H), 2.57 (brm, 4H), 2.40 (s, 3H), 2.23 (s, 3H). LCMS-2: t_R = 5.15. LCMS-5: t_R = 6.06. MS: *m/z* 397 $[M + H]^+$, expected 397 $[M + H]^+$.

***N*-[6-(3,5-Dimethylpyrazol-1-yl)-2-(5-methylfuran-2-yl)pyrimidin-4-yl]-2-[1,4]oxazepan-4-ylacetamide (10).** Intermediate **5** was reacted with homomorpholine according to the above general procedure. The product was purified by HPLC to give **10** as the TFA salt (light-brown oil, 85%). LCMS-3: t_R = 2.05. LCMS-5: t_R = 6.21. MS: *m/z* 411 $[M + H]^+$, expected 411 $[M + H]^+$.

***N*-[6-(3,5-Dimethylpyrazol-1-yl)-2-(5-methylfuran-2-yl)pyrimidin-4-yl]-2-(4-methoxypiperidin-1-yl)acetamide (11).** Intermediate **5** was reacted with 4-methoxypiperidine according to the above general procedure. The product was purified by HPLC to give **11** as the TFA salt (light-brown oil, 70%). LCMS-2: t_R = 5.40. LCMS-4: t_R = 10.23. MS: *m/z* 425 $[M + H]^+$, expected 425 $[M + H]^+$.

***N*-[6-(3,5-Dimethylpyrazol-1-yl)-2-(5-methylfuran-2-yl)pyrimidin-4-yl]-2-pyrrolidin-1-ylacetamide (12).** Intermediate **5** was reacted with pyrrolidine according to the above general procedure. The product was purified by HPLC to give **12** as the TFA salt (light-brown oil, 80%). ^{1}H NMR (300 MHz, $CDCl_3$): δ 7.52 (d, J = 3.6, 1H), 6.90 (s, 1H), 6.26 (d, J = 3.6, 1H), 6.06 (s, 1H), 2.77 (s, 3H),

2.47 (s, 3H), 2.29 (s, 3H), 0.08 (s, 1H). LCMS-2: $t_R = 5.20$. LCMS-5: $t_R = 6.36$. MS: m/z 381 $[M + H]^+$, expected 381 $[M + H]^+$.

2-((*S*)-3-Dimethylaminopyrrolidin-1-yl)-*N*-[6-(3,5-dimethylpyrazol-1-yl)-2-(5-methylfuran-2-yl)pyrimidin-4-yl]acetamide (13). Intermediate **5** was reacted with (*S*)-3-dimethylaminopyrrolidine according to the above general procedure. The product was purified by column on silica gel with DCM/methanol, 90/10, to give **13** as a white solid HCl salt (75%). ^{1}H NMR (300 MHz, DMSO-d_6): δ 8.30 (s, 1H), 7.21 (d, $J = 3.6$, 1H), 6.37 (d, $J = 3.6$, 1H), 6.22 (s, 1H), 2.00–4.05 (m, 9H), 2.83 (s, 6H), 2.73 (s, 3H), 2.39 (s, 3H), 2.23 (s, 3H). LCMS-6: $t_R = 16.50$. LCMS-7: $t_R = 30.06$. MS: m/z 424 $[M + H]^+$, expected 424 $[M + H]^+$.

2-((*R*)-3-Dimethylaminopyrrolidin-1-yl)-*N*-[6-(3,5-dimethylpyrazol-1-yl)-2-(5-methylfuran-2-yl)pyrimidin-4-yl]acetamide (14). Intermediate **5** was reacted with (*R*)-3-dimethylaminopyrrolidine according to the above general procedure. The product was purified by HPLC to give **14** as the TFA salt. ^{1}H NMR free base (300 MHz, $CDCl_3$): δ 9.57 (s, 1H), 8.47 (s, 1H), 7.16 (d, $J =$ 3.3 Hz, 1H), 6.16 (d, $J = 3.3$, 1H), 6.00 (s, 1H), 3.32 (AB syst, J = 10.5 Hz, 2H), 3.00–2.65 (m, 5H), 2.75 (s, 3H), 2.45 (s, 3H), 2.33 (s, 6H), 2.27 (s, 3H), 2.17–2.05 (m, 1H), 1.97–1.85 (m, 1H). LCMS-3: $t_R = 2.24$ (100%). LCMS-5: $t_R = 6.30$. MS: m/z 424 $[M + H]^+$, expected 424 $[M + H]^+$.

***N*-[6-(3,5-Dimethylpyrazol-1-yl)-2-(5-methylfuran-2-yl)pyrimidin-4-yl]-2-((*S*)-3-isopropoxypyrrolidin-1-yl)acetamide (15).** Intermediate **5** was reacted with (*S*)-3-hydroxypyrrolidine according to the above general procedure followed by a reaction with 2-bromopropane (1.2 equiv) and sodium hydride (1.1 equiv) in DMF at room temperature overnight. The product was purified by silica gel chromatography with DCM and 1% methanol as eluent. The HCl salt of **15** was obtained (17%). LCMS-5: $t_R = 6.35$. LCMS-2: $t_R = 5.85$. MS: m/z 439 $[M + H]^+$, expected 439 $[M + H]^+$.

***N*-[6-(3,5-Dimethylpyrazol-1-yl)-2-(5-methylfuran-2-yl)pyrimidin-4-yl]-2-((*R*)-3-ethylaminopyrrolidin-1-yl)acetamide (16).** Intermediate **5** was reacted with (*R*)-3-ethylaminopyrrolidine according to the above general procedure. The product was purified by column on silica gel with DCM/methanol, 90/10, and 1% NH_4OH to give **16** as a glassy solid (69 mg, 92%). ^{1}H NMR (300 MHz, $CDCl_3$): δ 9.65 (s, 1H), 8.45 (s, 1H), 7.15 (d, $J = 3.6$, 1H), 6.13 (d, $J = 3.6$, 1H), 5.99 (s, 1H), 3.65–3.71 (m, 1H), 3.38 (d, 2H), 2.98–3.10 (m, 4H), 2.99 (q, $J = 6.9$, 2H), 2.75 (s, 3H), 2.42 (s, 3H), 2.31–2.40 (m, 1H), 2.27 (s, 3H), 2.17–2.25 (m, 1H), 1.44 (t, $J = 6.9$, 3H). LCMS-3: $t_R = 2.17$. LCMS-4: $t_R = 10.06$. MS: m/z 424 $[M + H]^+$, expected 424 $[M + H]^+$.

***N*-[6-(3,5-Dimethylpyrazol-1-yl)-2-(5-methylfuran-2-yl)pyrimidin-4-yl]-2-((*S*)-3-ethylaminopyrrolidin-1-yl)acetamide (17).** Intermediate **5** was reacted with (*S*)-3-ethylaminopyrrolidine according to the above general procedure. The product was purified by column on silica gel with DCM/methanol, 90/10, to give **17** as a white solid HCl salt (35%). ^{1}H NMR (300 MHz, DMSO-d_6): δ 9.01 (s, 1H), 8.32 (s, 1H), 7.22 (d, $J = 3.3$, 1H), 6.38 (d, $J = 3.2$, 1H), 6.23 (s, 1H), 4.17 (m, 2H), 3.94 (bs, 4H), 3.41 (s, 1H), 3.00–3.02 (m, 2H), 2.73 (s, 3H), 2.39 (s, 3H), 2.23 (s, 3H), 2.09–2.18 (m, 2H), 1.20 (t, $J = 6.9$, 3H). LCMS-2: $t_R = 4.86$. LCMS-7: $t_R = 28.06$. MS: m/z 424 $[M + H]^+$, expected 424 $[M + H]^+$.

***N*-[6-(3,5-Dimethylpyrazol-1-yl)-2-(5-methylfuran-2-yl)pyrimidin-4-yl]-2-((*S*)-3-diethylaminopyrrolidin-1-yl)acetamide (18).** Intermediate **5** was reacted with (*S*)-3-diethylaminopyrrolidine according to the above general procedure. The product was purified by HPLC to give **18** as the TFA salt (light-brown oil, 60%). LCMS-2: $t_R = 4.92$. LCMS-5: $t_R = 5.99$. MS: m/z 452 $[M + H]^+$, expected 452 $[M + H]^+$.

General Method for Synthesis of Compounds 20−24: 2-(4-Dimethylaminomethylpiperidin-1-yl)-*N*-[6-(3,5-dimethylpyrazol-1-yl)-2-(5-methylfuran-2-yl)pyrimidin-4-yl]acetamide (22). To DMF (10 mL) were added intermediate **5** (760 mg, 2.2 mmol, 1 equiv), piperidin-4-ylmethylcarbamic acid *tert*-butyl ester (450 mg, 2.2 mmol, 1equiv), potassium carbonate (260 mg, 1 equiv), and a catalytic amount of TBAI. The reaction mixture was stirred at room temperature overnight. The reaction was quenched by addition of water (20 mL), stirred, and filtered. The Intermediate **19** was obtained as a white solid (1.1g, 96%). Alternatively, TEA or DIEA can be used as base. The white solid **19** was dissolved in dichloromethane (15 mL) followed by TFA (15 mL). The reaction mixture was stirred at room temperature for 2 h. The solvent was removed under nitrogen flow. The oil obtained was dissolved in EtOH (20 mL) and formaldehyde (20 mL, 30% in water), followed by borane−pyridine (2 mL) and 10 drops of acetic acid. The reaction mixture was stirred at room temperature overnight, then quenched with 1 M HCl (50 mL), stirred for 10 min, then neutralized by addition of sodium bicarbonate. The mixture was extracted with dichloromethane (2 × 100 mL). The organic layers were combined, dried (Na_2SO_4), concentrated, and purified by silica gel column, using dichloromethane (500 mL), followed by 10% methanol in dichloromethane (500 mL), and finally 10% 2 M ammonia in methanol in dichloromethane (1000 mL). Compound **22** was obtained as a clear oil (0.88 g, 93%). The oil was converted to the HCl salt via treatment with HCl in ether, followed by evaporation of the solvent and excess HCl to give compound **22** (HCl salt) as a light-yellow solid (0.9 g, 89%). ^{1}H NMR (300 MHz, $CDCl_3$): δ 9.49 (s, 1H), 8.47 (s, 1H), 7.18 (d, $J = 3.3$, 1H), 6.18 (d, $J = 3$, 1H), 6.01 (s, 1H), 3.17 (s, 2H), 2.97–2.93 (m, 4H), 2.85 (s, 6H), 2.77 (s, 3H), 2.47 (s, 3H), 2.28 (s, 3H), 1.91–1.87 (m, 2H), 1.70–1.55 (m, 5H). LCMS-6: $t_R = 15.87$. LCMS-7: $t_R = 35.09$. MS: m/z 452 $[M + H]^+$, expected 452 $[M + H]^+$.

2-((*R*)-3-Dimethylaminomethylpiperidin-1-yl)-*N*-[6-(3,5-dimethylpyrazol-1-yl)-2-(5-methylfuran-2-yl)pyrimidin-4-yl]acetamide (20). Compound **20** was obtained by the same method as compound **22**, using (*S*)-1-piperidin-3-ylmethylcarbamic acid *tert*-butyl ester instead of piperidin-4-ylmethylcarbamic acid *tert*-butyl ester. The title compound **20** (HCl salt) was obtained as a pale-yellow solid (0.22 g, 38%). ^{1}H NMR (300 MHz, $CDCl_3$) δ 9.56 (s, 1H), 8.47 (s, 1H), 7.17 (d, $J = 3.3$, 1H), 6.17 (d, $J = 3$, 1H), 6.01 (s, 1H), 3.22–2.84 (m, 6H), 2.76 (s, 3H), 2.72 (s, 6H), 2.44 (s, 3H), 2.28 (s, 3H), 2.14–2.12 (m, 2H), 1.82–1.18 (m, 5H). LCMS-6: $t_R = 15.76$. LCMS-7: $t_R = 36.21$ (100%). MS: m/z 452 $[M + H]^+$, expected 452 $[M + H]^+$.

2-((*S*)-3-Dimethylaminomethylpiperidin-1-yl)-*N*-[6-(3,5-dimethylpyrazol-1-yl)-2-(5-methylfuran-2-yl)pyrimidin-4-yl]acetamide (21). Compound **21** was obtained by the same method as compound **22**, using (*R*)-1-piperidin-3-ylmethylcarbamic acid *tert*-butyl ester instead of piperidin-4-ylmethylcarbamic acid *tert*-butyl ester. The title compound **21** was obtained as the HCl salt (0.25 g, 42%). ^{1}H NMR (300 MHz, $CDCl_3$): δ 9.57 (s, 1H), 8.46 (s, 1H), 7.16 (d, $J = 3.3$, 1H), 6.17 (d, $J = 3$, 1H), 6.00 (s, 1H), 3.30–2.81 (m, 6H), 2.76 (s, 3H), 2.72 (s, 6H), 2.43 (s, 3H), 2.27 (s, 3H), 2.14–2.12 (m, 2H), 1.82–1.18 (m, 5H). LCMS-6: $t_R = 15.58$. LCMS-7: $t_R = 36.22$. MS: m/z 452 $[M + H]^+$, expected 452 $[M + H]^+$.

2-((*R*)-3-Dimethylaminomethylpyrrolidin-1-yl)-*N*-[6-(3,5-dimethylpyrazol-1-yl)-2-(5-methylfuran-2-yl)pyrimidin-4-yl]acetamide (23). Compound **23** was obtained by the same method as compound **22**, using (*R*)-1-pyrrolidin-3-ylmethylcarbamic acid *tert*-butyl ester instead of piperidin-4-ylmethylcarbamic acid *tert*-butyl ester. The title compound **23** was obtained as the HCl salt (150 mg, 22%, from 500 mg of starting material). ^{1}H NMR (300 MHz, $CDCl_3$): δ 9.62 (s, 1H), 8.49 (s, 1H), 7.18 (d, $J = 3.3$, 1H), 6.17 (d, $J = 3$, 1H), 6.01 (s, 1H), 3.30 (d, $J = 5.4$, 2H), 2.91–2.69 (m, 4H), 2.69 (s, 3H), 2.45 (s, 3H), 2.50–2.28 (m, 3H), 2.33 (s, 6H), 2.28 (s, 3H), 2.20–1.55 (m, 2H). LCMS-6: $t_R = 15.10$. MS: m/z 438 $[M + H]^+$, expected 438 $[M + H]^+$. Anal. ($C_{23}H_{31}N_7O_2 \cdot 2HCl$) C,H, N.

2-((*S*)-3-Dimethylaminomethylpyrrolidin-1-yl)-*N*-[6-(3,5-dimethylpyrazol-1-yl)-2-(5-methylfuran-2-yl)pyrimidin-4-yl]acetamide (24). Compound **24** was obtained by the same method as compound **22**, using (*S*)-1-pyrrolidin-3-ylmethylcarbamic acid *tert*-butyl ester instead of piperidin-4-ylmethylcarbamic acid *tert*-butyl ester. The title compound was obtained as the HCl salt (350 mg, 51%, from 500 mg of starting material). ^{1}H NMR (300 MHz, $CDCl_3$): δ 9.62 (s, 1H), 8.49 (s, 1H), 7.18 (d, $J = 3.3$, 1H), 6.17 (d, $J = 3$, 1H), 6.01 (s, 1H), 3.30 (d, $J = 5.4$, 2H), 2.91–2.69 (m,

4H), 2.69 (s, 3H), 2.45 (s, 3H), 2.50–2.28 (m, 3H), 2.33 (s, 6H), 2.28 (s, 3H), 2.20–1.55 (m, 2H). LCMS-6: t_R = 15.12 (99%). MS: *m/z* 438 $[M + H]^+$, expected 438 $[M + H]^+$. Anal. ($C_{23}H_{31}N_7O_2 \cdot 2HCl$) C, H, N.

***N*-[6-(3,5-Dimethylpyrazol-1-yl)-2-(5-methylfuran-2-yl)pyrimidin-4-yl]acrylamide (25) for Compounds 26 and 27.** To intermediate **2** (1.0 g, 3.7 mmol, 1 equiv) stirring in 10 mL of DCM were added pyridine (0.389 mL, 4.8 mmol, 1.3 equiv) and acryloyl chloride (0.390 mL, 4.8 mmol, 1.3 equiv). The reaction mixture was stirred at room temperature overnight. The reaction was then quenched with saturated sodium bicarbonate (50 mL) and extracted with DCM (2 × 50 mL). The combined organic layers were dried ($MgSO_4$) and filtered to yield crude product **25** as a light-brown solid (80%), which was used without further purification. LCMS-1: t_R = 2.00. LCMS-2: t_R = 5.28. MS: *m/z* 324 $[M + H]^+$, expected 324 $[M + H]^+$.

3-Dimethylamino-*N*-[6-(3,5-dimethylpyrazol-1-yl)-2-(5-methylfuran-2-yl)pyrimidin-4-yl]propionamide (26). To intermediate **25** (0.80 g, 2.5 mmol, 1 equiv) stirring in DMF (2 mL) was added 2 M dimethylamine in THF (3.7 mL, 7.5 mmol, 3 equiv). The mixture was stirred at 40 °C for 2 h. The mixture from the completed reaction was diluted with brine (50 mL) and extracted with DCM (2 × 50 mL). The combined organic layers were dried ($MgSO_4$) and filtered to yield a light-brown oil. The crude product was purified by silica gel column using 10% methanol in dichloromethane. Compound **26** was obtained as a white solid (HCl salt) (75%). ^{1}H NMR (300 MHz, DMSO-d_6): δ 10.09 (bs, 1H), 8.33 (s, 1H), 7.20 (d, J = 3.3, 1H), 6.37 (dd, J = 3, 0.9, 1H), 6.22 (s, 1H), 3.37 (dd, J = 7.2, 12.3, 2H), 3.01 (dd, J = 6.9, 14.1, 2H), 2.79 (s, 3H), 2.77 (s, 3H), 2.72 (s, 3H), 2.39 (s, 3H), 2.22 (s, 3H). LCMS-6: t_R = 19.29. LCMS-7: t_R = 28.51. MS: *m/z* 369 $[M + H]^+$, expected 369 $[M + H]^+$. Anal. ($C_{19}H_{24}N_6O_2 \cdot 2HCl$) C, H, N.

3-((*S*)-3-Dimethylaminopyrrolidin-1-yl)-*N*-[6-(3,5-dimethylpyrazol-1-yl)-2-(5-methylfuran-2-yl)pyrimidin-4-yl]propionamide (27). Compound **27** was prepared in a fashion similar to that for compound **25** using (3*S*)-(−)-3-(dimethylamino)pyrrolidine in place of dimethylamine. Compound **27** was obtained as a white solid (HCl salt) (78%). ^{1}H NMR (300 MHz, DMSO-d_6): δ 8.34 (s, 1H), 7.19 (d, J = 2.7, 1H), 6.35 (d, J = 2.7, 1H), 6.20 (s, 1H), 4.15 (brm, 4H), 3.50 (brm, 5H), 2.99 (m, 2H), 2.84 (s, 6H), 2.72 (s, 1H), 2.38 (s, 1H), 2.21 (s, 1H). LCMS-6: t_R = 15.11. LCMS-7: t_R = 29.43. MS: *m/z* 438 $[M + H]^+$, expected 438 $[M + H]^+$. Anal. ($C_{23}H_{31}N_7O_2 \cdot 3HCl$) C, H, N.

Biology Experimental Section. Pharmacology. Adenosine A_1 and A_{2A} Receptor Binding Assays. Receptor Cloning. The coding sequence of the human A_1 and A_{2A} receptor was amplified from a human brain cDNA library by the polymerase chain reaction. Each amplicon was cloned into the pcDNA5/FRT/V5-His-TOPO expression vector (Invitrogen) and sequence confirmed using an ABI 3100 automated sequencer (Applied Biosystems). Each expression construct was transfected into Flp-In HEK cells (Invitrogen) using Lipofectamine 2000 (Invitrogen). Cells stably expressing either the human A_1 or A_{2A} receptor were selected using 1 mg/mL hygromycin in complete DMEM.

Membrane Preparation. Crude membranes were prepared from Flp-In HEK cells transfected with either the human A_1 or A_{2A} receptor by resuspending cells in lysis buffer (50 mM Tris-HCl, pH 7.4, 5 mM EDTA, 10 mM $MgCl_2$) and disrupting under N_2 at a pressure of 900 psi (Parr cell disruption bomb, catalog no. 4639) for 30 min on ice followed by differential centrifugation. The resulting crude membrane pellet was resuspended in assay buffer (50 mM Tris-HCl, pH 7.4, 1 mM EDTA, 10 mM $MgCl_2$). Membrane protein concentration was determined by Bradford assay. Membranes of cloned rat A_{2A} receptor produced in CHO cells were obtained from Perkin-Elmer (SignalScreen lot no. 6110536-09). Membrane aliquots were stored at −80 °C.

Binding Assay. An aliquot of membranes (1–2 μg of protein) was preincubated for 30 min at room temperature in the presence of 10 μg/mL adenosine deaminase (type IV calf spleen, Sigma). Membranes were then incubated for 90 min with either 1.0 nM [^{3}H]-DPCPX (120.00 Ci/mmol PerkinElmer NET 974) for the A_1 membranes or 2.0 nM [^{3}H]-ZM 241385 (27.40 Ci/mmol Tocris R1036) for the A_{2A} human and rat membranes in the presence of varying concentrations of competing ligand. Nonspecific binding was determined in the presence of excess (1 μM) of DPCPX or CGS15943 for the A_1 and A_{2A} membranes, respectively. Bound and free ligands were separated by rapid vacuum filtration using a Packard 96-well cell harvester onto UniFilter GF/C filter plates (PerkinElmer) that had been pretreated with 0.5% polyethyleneimine. The filter plates were than washed 3 × 200 μL with 50 mM Tris-HCl and 50 mM NaCl, pH 7.4. Bound radioligand was determined by scintillation counting using a TopCount-NXT (Packard). Binding data were analyzed by nonlinear, least-squares curve-fitting algorithms using GraphPad Prism (GraphPad Software, Inc., San Diego, CA) or ActivityBase (IDBS, Guildford, Surrey, U.K.). K_i values were calculated from IC_{50} values using the Cheng−Prusoff equation (Cheng and Prusoff, 1973).[9] (1) For the A_1 membrane assay, the results are as follows: [^{3}H]-DPCPX measured K_d = 1.0 ± 0.5 nM; B_{max} = 8 ± 4 pmol/mg by Scatchard analysis; control DPCPX (Tocris, 0439) K_i = 1.6 ± 0.7 nM. (2) For the human A_{2A} membrane assay, the results are as follows: [^{3}H]-ZM241385 measured K_d = 0.22 ± 0.20 nM; B_{max} = 33 ± 8 pmol/mg by Scatchard analysis; control NBI 80634 K_i = 0.25 ± 0.04 nM. (3) For the rat A_{2A} membrane assay, the results are as follows: [^{3}H]-ZM241385 measured K_d = 0.33 ± 0.20 nM; B_{max} = 2.4 pmol/mg by Scatchard analysis; control NBI 80634 K_i = 1.2 ± 0.3 nM.

hERG Assay Protocol. Overview. Compounds that inhibit hERG potassium channels have been shown to prolong the QT interval of the ECG in man and increase the risk of cardiac arrhythmias (Ficker et al., 1998; Kiehn et al., 1996; Mohammad et al., 1997). A preclinical assay was used to determine whether drug candidates inhibit hERG by examining their ability to block the potassium tail currents in HEK293 cells stably transfected with hERG cDNA (Zhou et al., 1997; Zhou et al., 1998). Concentration–response curves for test compounds were generated and the maximum inhibition and IC_{50} value determined.[10]

Source and Maintenance of hERG Transfected Cells. hERG. T.HEK (HEK293 cells stably transfected with hERG cDNA) were obtained from the University of Wisconsin. The cells were continuously maintained and passaged in minimum essential medium (MEM) supplemented with 10% fetal bovine serum, 1% nonessential amino acids, and 0.4 mg/ml Geneticin (Gibco-BRL). For electrophysiology studies, the cells were plated onto sterile glass coverslips in 24-well tissue culture trays (containing 0.5 mL medium) at a density (2000–5000 cells per well) that enabled isolated cells to be selected for patch clamping. The dishes were stored in a humidified, gassed (7.5% CO_2) incubator at 37 °C.

Electrophysiological Assay Protocol. Coverslips, upon which cells had been plated, were transferred to the recording chamber on an inverted microscope and continuously perfused (1–2 mL/min) with control solution at room temperature. Test substances were applied by bath perfusion, switching from the control solution to one containing the appropriate concentration of test substance. The recording chamber volume was approximately 0.5 mL, and fluid exchange took approximately 1 min.

The hERG current was recorded using standard patch-clamp methods. A schematic diagram of the voltage waveform used in these experiments is indicated below. The standard voltage profile was as follows: (1) V_{step} from −80 to −50 mV for 0.5 s to determine holding current, (2) V_{step} from −50 to +10 mV for 4 s to activate hERG current, (3) V_{step} from +10 to −50 mV for 4 s to remove voltage-dependent inactivation and elicit the hERG tail current, and (4) return to the holding potential of −80 mV. The voltage waveform was repeated every 12 s (one trial), and the current responses to each waveform were digitized and stored onto a computer hard disk.

The baseline hERG tail current was recorded for at least 5 min (25 trials at 12 s intervals) in control bath solution to assess the suitability and stability of the cell. Once a stable baseline hERG tail current had been established, the test substance at the lowest concentration (0.1 nM) was applied for 5 min. Then the test

substance was washed out by reperfusing with the control bath solution for at least 5 min or until the effect was completely reversed. When the new baseline hERG tail current was established (typically 5 min), the next highest concentration of test substance was applied for 5 min and washed out for at least 5 min. This was repeated until the highest concentration of test substance had been tested. Concentrations of 0.1 nM to 10 μM were used to determine the concentration–response relationship of test substances. This was performed on 2–6 cells/concentration.

The peak tail current amplitude from each trial was measured off-line from the digitized data files using PClamp 9 software and entered into an Excel spreadsheet. The concentration–response data (normalized to predrug baseline) was plotted and fitted to a sigmoidal function (logistic four parameter) using SigmaPlot software. The IC_{50} value was derived from the fitted curve.

Preclinical Assays. Metabolic Stability Assay in Rat and Human Liver Microsomes. Pooled male human and rat liver microsomes (0.5 mg/mL for human and 0.1 mg/mL for rat; $n >$ 10; mixed gender) were incubated at 37 °C with the NCE in the presence of an NADPH-generating system containing 50 mM, pH 7.4, potassium phosphate buffer, 3 mM magnesium chloride, 1 mM EDTA, 1 mM NADP, 5 mM G-6-P, and 1 unit/mL G-6-PD. Incubations were conducted with 1 μM of each NCE (0.01% DMSO) with a total volume of 250 μL, in duplicate at each time point (0, 5, 10, 20, 40, and 60 min). Reactions were stopped by the addition of 0.3 mL of acetonitrile containing a proprietary internal standard. Precipitated proteins were removed by centrifugation for 15 min at 3000 rpm, and the supernatant fluid (~0.1 mL) was analyzed by LCMS for the percentage of parent compound remaining. The in vitro initial rates of metabolism were scaled using constants, such as microsomal protein/g of liver, g of liver/kg of body weight, and liver blood flow, to predict systemic clearance and maximum predicted percent bioavailability. These calculations from nonlinear regression assume that liver metabolism alone is the determinant of bioavailability.

Metabolite Identification Assay in Human Liver Microsomes. Human liver microsomes (HLM) were purchased from a commercial source (XenoTech LLC, Kansas City, KS) as a mixed gender pool from 10 donors. Liver microsomal incubations for metabolite identification were conducted using a 50 μM concentration of the NCE at a microsomal protein concentrations of 0.5 mg/mL in a 50 mM potassium phosphate buffer in the presence of an NADPH-generating system composed of 1.0 mM NADP+, 3.0 mM $MgCl_2$, 5.0 mM G6P, and 3.0 units/mL G6PDH. A 50 mM stock solution of the NCE in DMSO was used to achieve a final concentration 50 μM, with the final concentration of DMSO being less than 0.1% v/v. All concentrations are relative to a final incubation volume of 1 mL.

Incubations were conducted for 0, 30, 60, and 120 min at 37 °C in a shaking water bath and were terminated by adding 1 mL of ice-cold ACN. After the incubation suspensions are thoroughly vortexed for 1 min and centrifuged at 3000 rpm for 20 min, and the resultant supernatant fractions were kept at −80 °C before LCMS analysis.

LCMS analysis was carried out on an Agilent 1100 LC system coupled to a Finnigan LCQ ion trap mass spectrometer. The Agilent 1100 LC systems consisted of a binary pump, a diode array detector, a column heater, and a vacuum degasser/mobile phase tray. The LC columns were typically a YMC ODS-AQ column, 150 mm × 2 mm i.d. and 5 μm particle size, and were operated at 45 °C. A typical mobile phase used consisted of mobile phase A (0.1% formic acid in deionized water) and mobile phase B (0.1% formic acid in acetonitrile). Gradients were generally about 25 min long and were optimized for separation of each NCE and its metabolites. Flow rates were typically 0.40 mL/min. The mass spectrometer was operated in (+)-ESI mode, and data dependent MS−MS spectra were obtained for structural characterization.

In Human Liver Hepatocytes. Human hepatocytes were purchased from a commercial source (XenoTech LLC, Kansas City, KS). Cryopreservation vials containing hepatocytes are removed from the liquid nitrogen storage unit and quickly placed in a water bath at 37 °C for 2.0 min. Hepatocytes are prepared with hepatocyte isolation kit (XenoTech LLC) according to the protocol provided by the manufacture (see manufacturer's appendix). Contents of the cryopreservation vials are gently poured into tube A containing Percoll solution and rinsed with 1.67 mL of tube B. The cell suspension is mixed by gentle inversion and centrifuged at 500–700 rpm for 5 ± 0.5 min at room temperature. The cell pellets are gently resuspended with 5 mL of tube B by inversion. The viability of hepatocytes is recorded. The volume of cell suspension is adjusted with tube B to obtain a cell concentration of approximately 1.0×10^6 to 4.0×10^6 cells/mL. The cell suspension is centrifuged again at 400–600 rpm for 3 ± 0.5 min at room temperature. The cell pellets are gently resuspended with 2 mL Krebs Henseleit buffer (Sigma) by inversion. The cells suspension is adjusted with Krebs Henseleit buffer to get a cell concentration of approximately 2.5×10^6 cells/mL. If rat hepatocytes are used or the incubation time is over 2 h, it is suggested that Waymouth's medium be used instead of Krebs Henseleit buffer.

In Vivo HIC Assay. Selected compounds were tested for their effects on haloperidol-induced catalepsy measured with the bar test. Separate groups of rats were used to test each compound ($n = 24$/experiment). Male Wistar rats (Charles River) were habituated to the vivarium for 1 week prior to testing. Rats were weighed (~220 g at time of testing) and administered test compound orally (po) 2 h prior to the bar test. The vehicle for all test compounds was 5% cremophor in sterile water given at a volume of 5 mL/kg. One hour prior to the bar test, rats were given an intraperitoneal (ip) injection of haloperidol (1.5 mg/kg in a 10 mL/kg sterile water). The bar test consisted of three 30 s trials spaced 3 min apart. During a test, the rat's forepaws were placed on an 8.0 cm high metal bar. The descent latency of one paw from the bar was measured and recorded (in seconds) as the score for a given trial. The descent latency from each of the three trials was averaged to obtain the mean descent latency for each rat. Plasma and brain samples were collected following the haloperidol-induced catalepsy test (samples collected 2 h after dose), and samples were analyzed to determine exposure (method described below in the screening PK protocol section).

Screening PK Protocol for Sample Extraction and Analysis To Determine Brain Exposure in Rat at the 2 h Time Point. Brain Sample Extraction. Brain tissue sample analysis was conducted by liquid chromatography in tandem with a mass spectrometric detection (LC−MS/MS) method. Half of the brain (left or right) was weighed and homogenized in 2.0 mL of ACN/H_2O/FA (formic acid) (v/v: 60/40/0.1) containing 50 μL of a proprietary internal standard (10 μg/mL NBI-67377). The homogenates were centrifuged at 3000 rpm for 20 min, and the supernatant was collected for LC−MS/MS analysis. Brain standards were prepared by spiking 1.0 mL of a series of premade calibration standard aqueous solutions (prepared in 60/40 ACN/H_2O), 1.0 mL of ACN/H_2O/FA (v/v: 60/40/0.2), and 50 μL of internal standard (10 μg/mL) into half of a rat brain. Standards for brain were processed and analyzed at the same time and in exactly the same way as the analytical samples.

Bioanalysis. The LC−MS/MS system equipped with Agilent 1100 HPLC system was coupled to a CTC PAL autoinjector (Leap Technologies, Carrboro, NC) and a Sciex API 4000 triple quadruple mass spectrometer. Samples were eluted at 0.45 mL/min using a mobile phase consisting of solution A (0.1% formic acid in water) and solution B (0.1% formic acid in acetonitrile) with a fast gradient (0–0.1 min, 5% B; 0.1–1.0 min, 5−95% B; hold to 2.5 min; 2.5–2.7 min, 95–5% B; hold to 3.5 min) and a column temperature of 20 °C. The HPLC column used for this assay was Agilent Zorbax SB-C18 column, 2.1 mm × 50 mm, with a particle size of 5 μm. Electrospray ionization source was used for detection at a positive MRM (multiple reaction monitoring) mode. Quantification was performed by fitting peak area ratios (peak of parent analyte vs peak of the internal standard) to a weighted ($1/x$) linear calibration curve.

Acknowledgment. We thank Shawn Ayube, Paddi Ekhlassi, and John Harman for analytical support.

Supporting Information Available: Copies of NMR and LCMS data are available on key final compounds. This material is available free of charge via the Internet at http://pubs.acs.org.

References

(1) (a) Dutta, A. K.; Le, W. Existing dopaminergic therapies for Parkinson's disease. *Expert Opin. Ther. Patents* **2006**, *16*, 1613–1625. (b) Foley, P.; Gerlach, M.; Double, K. L.; Riederer, P. Dopamine receptor agonists in the therapy of Parkinson's disease. *J. Neural Transm.* **2004**, *111*, 1375–1446. (c) Ahlskog, J. E.; Muenter, M. D. Frequency of levodopa-related dyskinesias and motor fluctuations as estimated from the cumulative literature. *Mov. Disord.* **2001**, *16*, 448–458. (d) Rascol, O.; Brooks, D. J.; Korczyn, A. D.; De Deyn, P. P.; Clarke, C. E.; Lang, A. E. A five-year study of the incidence of dyskinesia in patients with early Parkinson's disease who were treated with ropinirole or levodopa. 056 Study Group. *N. Engl. J. Med.* **2000**, *342*, 1484–1491. (e) Marsden, C. D.; Parkes, J. D. "On−off" effects in patients with Parkinson's disease on chronic levodopa therapy. *Lancet* **1976**, *1*, 292–296.

(2) (a) Xu, K.; Bastia, E.; Schwarzschild, M. Therapeutic potential of adenosine A_{2A} receptor antagonists in Parkinson's disease. *Pharmacol. Ther.* **2005**, *105*, 267–310. (b) Jenner, P. Istradefylline, a novel adenosine A_{2A} receptor antagonist, for the treatment of Parkinson's disease. *Expert Opin. Invest. Drugs* **2005**, *14*, 729–738. (c) Bara-Jimenez, W.; Sherzai, A.; Dimitrova, T.; Favit, A.; Bibbiani, F.; Gillespie, M.; Morris, M. J.; Mouradian, M. M.; Chase, T. N. Adenosine receptor antagonist treatment of Parkinson's disease. *Neurology* **2003**, *61*, 293–296. (d) Hauser, R. A.; Hubble, J. P.; Truong, D. D. Randomized trial of the adenosine A_{2A} antagonist istradefylline in advanced PD. *Neurology* **2003**, *61*, 297–303. (e) Kase, H.; Aoyama, S.; Ichimura, M.; Ikeda, K.; Ishii, A.; Kanda, T.; Koga, K.; Koike, N.; Kurokawa, M.; Kuwana, Y.; Mori, A.; Nakamura, J.; Nonaka, H.; Ochi, M.; Saki, M.; Shimada, J.; Shindou, T.; Shiozaki, S.; Suzuki, F.; Takeda, M.; Yanagawa, K.; Richardson, P. J.; Jenner, P.; Bedard, P.; Borrelli, E.; Hauser, R. A.; Chase, T. N. Progress in the pursuit of therapeutic A_{2A} antagonists: the adenosine A_{2A} receptor selective antagonist KW-6002: research and development toward a novel nondopaminergic therapy for Parkinson's disease. *Neurology.* **2003**, *61* (11, Suppl. 6), S97–S100.

(3) (a) Xiao, D.; Bastia, E.; Xu, Y. H.; Benn, C. L.; Cha, J. H. J.; Peterson, T. S.; Chen, J. F.; Schwarzschild, M. A. Forebrain adenosine A_{2A} receptors contribute to L-3,4-dihydroxyphenylalanine-induced dyskinesia in hemiparkinsonian mice. *J. Neurosci.* **2006**, *26*, 13548–13555. (b) Calon, F.; Dridi, M.; Hornykiewicz, O.; Bedard, P. J.; Rajput, A. H.; Di Paolo, T. Increased adenosine A_{2A} receptors in the brain of Parkinson's disease patients with dyskinesias. *Brain* **2004**, *127*, 1075–1084. (c) Kanda, J.; Jackson, M. J.; Smith, L. A.; Pearce, R. K.; Nakamura, J.; Kase, H.; Kuwana, Y.; Jenner, P. Combined use of the adenosine A_{2A} antagonists KW-6002 with L-DOPA or with selective D1 or D2 dopamine agonists, increases antiparkinsonian activity but not dyskinesia in MPTP-treated monkeys. *Exp. Neurol.* **2000**, *162*, 321–327. (d) Kanda, T.; Jackson, M. J.; Smith, L. A.; Pearce, R. K.; Nakamura, J.; Kase, H.; Kuwana, Y.; Jenner, P. Adenosine A_{2A} antagonist: a novel antiparkinsonian agent that does not provoke dyskinesia in parkinsonian monkeys. *Ann. Neurol.* **1998**, *43*, 507–13.

(4) (a) Huang, Z. L.; Qu, W. M.; Eguchi, N.; Chen, J. F.; Schwarzschild, M. A.; Fredholm, B. B.; Urade, Y.; Hayaishi, O. Adenosine A_{2A}, but not A1, receptors mediate the arousal effect of caffeine. *Nat. Neurosci.* **2005**, *8*, 858–859. (b) Basheer, R.; Strecker, R. E.; Thakker, M. M.; McCarley, R. W. Adenosine and sleep−wake regulation. *Prog. Neurobiol.* **2004**, *73*, 379–396. (c) Urade, Y.; Eguchi, N.; Qu, W. M.; Sakata, M.; Huang, Z. L.; Chen, J. F.; Schwarzschild, M. A.; Fink, J. S.; Hayaishi, O. Sleep regulation in adenosine A_{2A} receptor-deficient mice. *Neurology* **2003**, *61*, S94–S96.

(5) (a) Kalda, A.; Yu, L.; Oztas, E.; Chen, J. F. Novel neuroprotection by caffeine and adenosine A(2A) receptor antagonists in animal models of Parkinson's disease. *J. Neurol. Sci.* **2006**, *248*, 9–15. (b) Pierri, M.; Vaudano, E.; Sager, T.; Englund, U. KW-6002 protects from MPTP-induced dopaminergic toxicity in the mouse. *Neuropharmacology* **2005**, *48*, 517–524. (c) Ikeda, K.; Kurokawa, M.; Aoyama, K. Y. Neuroprotection by adenosine A_{2A} receptor blockade in experimental models of Parkinson's disease. *J. Neurochem.* **2002**, *80*, 262–270. (d) Popoli, P.; Pintor, A.; Domenici, M. R.; Frank, C.; Tebano, M. T.; Pezzola, A.; Scarchilli, L.; Quarta, D.; Reggio, R.; Malchiodi-Albedi, F.; Falchi, M.; Massotti, M. Blockade of striatal adenosine A_{2A} receptor reduces, through a presynaptic mechanism, quinolinic acid-induced excitotoxicity: possible relevance to neuroprotective interventions in neurodegenerative diseases of the striatum. *J. Neurosci.* **2002**, *22*, 1967–1975. (e) Chen, J. F.; Xu, K.; Petzer, J. P.; Stall, R.; Xy, Y. H.; Beilstein, M.; Sonsalla, P. K.; Castagnoli, K.; Castagnoli, N., Jr.; Schwarzschild, M. A. Neuroprotection by caffeine and A_{2A} adenosine receptor inactivation in a model of Parkinson's disease. *J. Neurosci.* **2001**, *21*, 1–6. (f) Chen, J. F.; Huang, Z.; Ma, J.; Zhu, J.; Moratella, R.; Standaert, D.; Moskowitz, M. A.; Fink, J. S.; Schwarzschild, M. A. A_{2A} adenosine receptor deficiency attenuates brain injury induced by transient focal ischemia in mice. *J. Neurosci.* **1999**, *19*, 9192–9200. (g) Monopol, A.; Lozza, G.; Forlani, A.; Mattavelli, A.; Ongini, E. Blockade of adenosine A_{2A} receptors by SCH 58261 results in neuroprotective effects in cerebral ischemia in rats. *NeuroReport* **1998**, *9*, 3955–3959.

(6) Slee, D. H.; Chen, Y.; Zhang, X.; Moorjani, M.; Lanier, M. C.; Lin, E.; Rueter, J. K.; Williams, J. P.; Lechner, S. M.; Markison, S.; Malany, S.; Santos, M.; Jalali, K.; Wen, J.; O'Brien, Z.; Castro-Palomino, J. C.; Crespo, M. I.; Prat, M.; Gual, S.; Diaz, J. L.; Saunders, J. 2-Amino-*N*-pyrimidin-4-ylacetamides as A_{2A} receptor antagonists. 1. SAR and optimization of heterocyclic substituents. *J. Med. Chem.* **2008**, *51*, 1719–1729.

(7) (a) Collins, I.; Rowley, M.; Davey, W. B.; Emms, F.; Marwood, R.; Patel, S.; Patel, S.; Fletcher, A.; Ragan, I. C.; Leeson, P. D.; et al. 3-(1-Piperazinyl)-4,5-dihydro-1*H*-benzo[*g*]indazoles: high affinity ligands for the human dopamine D_4 receptor with improved selectivity over ion channels. *Bioorg. Med. Chem.* **1998**, *6*, 743–753. (b) Bourrain, S.; Collins, I.; Neduvelil, J. G.; Rowley, M.; Leeson, P. D.; Patel, S.; Patel, S.; Emms, F.; Marwood, R.; Chapman, K. L.; et al. Substituted pyrazoles as novel selective ligands for the human dopamine D_4 receptor. *Bioorg. Med. Chem.* **1998**, *6*, 1731–1743. (c) Rowley, M.; Hallett, D. J.; Goodacre, S.; Moyes, C.; Crawforth, J.; Sparey, T. J.; Patel, S.; Marwood, R.; Patel, S.; Thomas, S.; Hitzel, L.; O'Connor, D.; Szeto, N.; Castro, J. L.; Hutson, P. H.; MacLeod, A. M. 3-(4-Fluoropiperidin-3-yl)-2-phenylindoles as high affinity, selective, and orally bioavailable h5-HT_{2A} receptor antagonists. *J. Med. Chem.,* **2001**, *44*, 1603–1614. (d) Fletcher, S. R.; Burkamp, F.; Blurton, B.; Cheng, S. K. F.; Clarkson, R.; O'Connor, D.; Spinks, D.; Tudge, M.; van Niel, M. B.; Patel, S.; Chapman, K.; Marwood, R.; Shepheard, S.; Bentley, G.; Cook, G. P.; Bristow, L. J.; Castro, J. L.; Hutson, P. H.; MacLeod, A. M. 4-(Phenylsulfonyl)piperidines: novel, selective, and bioavailable 5-HT_{2A} receptor antagonists. *J. Med. Chem.* **2001**, *45*, 492–503. (e) Matasi, J. J.; Caldwell, J. P.; Zhang, H.; Fawzi, A.; Higgins, G. A.; Cohen-Williams, M. E.; Varty, G. B.; Tulshian, D. B. 2-(2-Furanyl)-7-phenyl[1,2,4]triazolo[1,5-*c*]pyrimidin-5-amine analogs as adenosine A_{2A} antagonists: The successful reduction of hERG activity. Part 2. *Bioorg. Med. Chem. Lett.* **2005**, *15*, 3675–3678. (f) Bell, I. M.; Gallicchio, S. N.; Abrams, M.; Beshore, D. C.; Buser, C. A.; Culberson, J C.; Davide, J.; Ellis-Hutchings, M.; Fernandes, C.; Gibbs, J. B.; Graham, S. L.; Hartman, G. D.; Heimbrook, D. C.; Homnick, C. F.; Huff, J. R.; Kassahun, K.; Koblan, K. S.; Kohl, N. E.; Lobell, R. B.; Lynch, J. J., Jr,; Miller, P. A.; Omer, C. A.; Rodrigues, A. D.; Walsh, E. S.; Williams, T. M. Design and biological activity of (*S*)-4-(5-{[1-(3-chlorobenzyl)-2- oxopyrrolidin-3-ylamino]methyl}imidazol-1-ylmethyl)benzonitrile, a 3-aminopyrrolidinone farnesyltransferase inhibitor with excellent cell potency. *J. Med. Chem.,* **2001**, *44*, 2933–2949. (g) Potet, F.; Bouyssou, T.; Escande, D.; Baro, I. Gastrointestinal prokinetic drugs have different affinity for the human cardiac human ether-a-gogo K(+) channel. *J. Pharmacol. Exp. Ther.* **2001**, *299*, 1007–1112.

(8) Weiss, S. M.; Benwell, K.; Cliffe, I. A.; Gillespie, R. J.; Knight, A. R.; Lerpiniere, J.; Misra, A.; Pratt, R. M.; Revell, D.; Upton, R.; Dourish, C. T. Discovery of nonxanthine adenosine A_{2A} receptor antagonists for the treatment of Parkinson's disease. *Neurology* **2003**, *61*, S101–S106.

(9) Cheng, Y.; Prusoff, W. H. Relationship between the inhibition constant (K1) and the concentration of inhibitor which causes 50% inhibition (I50) of an enzymatic reaction. *Biochem. Pharmacol.* **1973**, *22*, 3099–3108.

(10) (a) Ficker, E.; Jarolimek, W.; Kiehn, J.; Baumann, A.; Brown, A. M. Molecular determinants of dofetilide block of HERG K^+ channels. *Circ. Res.* **1998**, *82*, 386–395. (b) Kiehn, J.; Lacerda, A. E.; Wible, B.; Brown, A. M. Molecular physiology and pharmacology of HERG. Single-channel currents and block by dofetilide. *Circulation* **1996**, *94*, 2572–2579. (c) Mohammad, S.; Zhou, Z.; Gong, Q.; January, C. T. Blockage of the HERG human cardiac K^+ channel by the gastrointestinal prokinetic agent cisapride. *Am. J. Physiol.* **1997**, *273*, H2534–H2538. (d) Zhou, Z.; Gong, Q.; Ye, B.; Fan, Z.; Makielski, J. C.; Robertson, G. A.; January, C. T. Electrophysiological and Pharmacological Properties of HERG channels in a stably transfected human cell line (Abstract). *Biophys. J.* **1997**, *72*, A225. (e) Zhou, Z.; Gong, Q.; Ye, B.; Fan, Z.; Makielski, J. C.; Robertson, G. A.; January, C. T. Properties of HERG channels stably expressed in HEK 293 cells studied at physiological temperature. *Biophys. J.* **1998**, *74*, 230–241.

JM701187W